

## Research Article

# Growth of Horizontal Nanopillars of CuO on NiO/ITO Surfaces

Siddharth Joshi,<sup>1</sup> Mrunmaya Mudigere,<sup>1,2</sup> L. Krishnamurthy,<sup>1,2</sup> and G. L. Shekar<sup>1,3</sup>

<sup>1</sup> Centre of Nanotechnology, National Institute of Engineering, Mysore, Karnataka 570008, India

<sup>2</sup> Department of Mechanical Engineering, National Institute of Engineering, Mysore, Karnataka 570008, India

<sup>3</sup> Department of Industrial Production Engineering, National Institute of Engineering, Mysore, Karnataka 570008, India

Correspondence should be addressed to Siddharth Joshi; [siddharth\\_joshi@hotmail.com](mailto:siddharth_joshi@hotmail.com)

Received 30 January 2014; Revised 6 August 2014; Accepted 7 August 2014; Published 28 August 2014

Academic Editor: Kui-Qing Peng

Copyright © 2014 Siddharth Joshi et al. This is an open access article distributed under the Creative Commons Attribution License, which permits unrestricted use, distribution, and reproduction in any medium, provided the original work is properly cited.

We have demonstrated hydrothermal synthesis of rectangular pillar-like CuO nanostructures at low temperature ( $\sim 60^\circ\text{C}$ ) by selective growth on top of NiO porous structures film deposited using chemical bath deposition method at room temperature using indium tin oxide (ITO) coated glass plate as a substrate. The growth of CuO not only filled the NiO porous structures but also formed the big nanopillars/nanowalls on top of NiO surface. These nanopillars could have significant use in nanoelectronics devices or can also be used as p-type conducting wires. The present study is limited to the surface morphology studies of the thin nanostructured layers of NiO/CuO composite materials. Structural, morphological, and absorption measurement of the CuO/NiO heterojunction were studied using state-of-the-art techniques like X-ray diffraction (XRD), transmission electron microscopy (SEM), atomic force microscopy (AFM), and UV spectroscopy. The CuO nanopillars/nanowalls have the structure in order of  $(5 \pm 1.0) \mu\text{m} \times (2.0 \pm 0.3) \mu\text{m}$ ; this will help to provide efficient charge transport in between the different semiconducting layers. The energy band gap of NiO and CuO was also calculated based on UV measurements and discussed.

## 1. Introduction

In the modern society, environmental and energy resource concerns have been increasing, and because of that, greater stress has been placed on development of renewable energy resources especially on solar energy based photovoltaic cells, whose economic feasibility relies on efficient collection, retention, and utilization of photons. Over the past decade, research on solar cell has become one of the hot topics within science and engineering [1–3]. The need for higher solar cell efficiencies at lower cost has become apparent, and at the same time synthetic control of nanostructures using top-down/bottom-up approaches has improved such that the high performance electronic devices are becoming possible [4, 5]. Inorganic nanostructures [6] with tailored geometry over their organic counterparts are expected to play significant roles for the next-generation nanoscale electronic, optoelectronic, electrochemical, and electromechanical devices [7–10].

Copper oxides (CuO and  $\text{Cu}_2\text{O}$ ) are p-type semiconductor oxides, suitable materials for high efficiency solar cells due

to their band gap of 1.3 and 2.0 eV, respectively, which are close to the ideal energy gap for solar cells, and well matched with the solar spectrum. CuO has been intensively studied for photovoltaic/sensing devices due to its rich family of nanostructures and promising electrochemical and catalytic properties it possesses at nanoscale level [11–13]. From the literature, CuO nanostructures can be grown on a Cu substrate using a thermal oxidation process or synthesized through wet chemical routes especially using hydrothermal method on any supporting substrates, whereas CuO nanostructures (NS) grown by wet chemical method show poor adhesion to the substrates [13]. Therefore, under present work, the substrate has been modified by predeposition of NiO porous layer on top of ITO/glass substrate, which is expected to enhance the adhesion of CuO nanostructure on top of NiO porous layer.

At the same time, synthesis of nanomaterials using hydrothermal method has come up as a cost effective method for producing the different CuO nanostructures on flexible substrates [14]. By applying the hydrothermal approach one can be able to precisely gain control over the synthesis of the nanocorals (NCs) consisting of p-type CuO at low

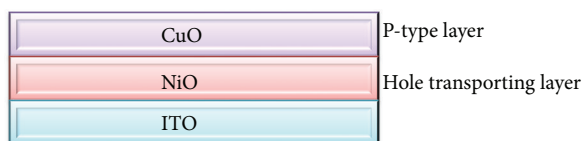


FIGURE 1: Schematic side view of ITO/NiO/CuO three-layer system.

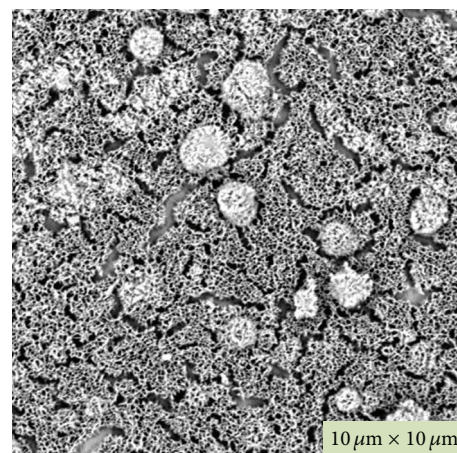
temperature. This is achieved by assembling hierarchical CuO NC from a single-precursor entity (copper nitrate) at 60°C. The important features of copper oxide semiconductors are high optical absorption coefficient and nontoxicity and low cost fabrication [15, 16].

The present paper deals with the horizontal pillar-like nanostructured formation of CuO layer on top of NiO porous layer modified ITO/glass substrate. Reasons of using NiO layer could be firstly to provide better surface interface interaction with CuO and this will ultimately improve the adhesion property of CuO on modified substrate (NiO/ITO/glass) and secondly the device aspect as NiO layer can act as hole transporting layer too. The schematic side view layer structure has been shown in Figure 1. For any device application further, any n-type layer can be deposited to form the pn-junction.

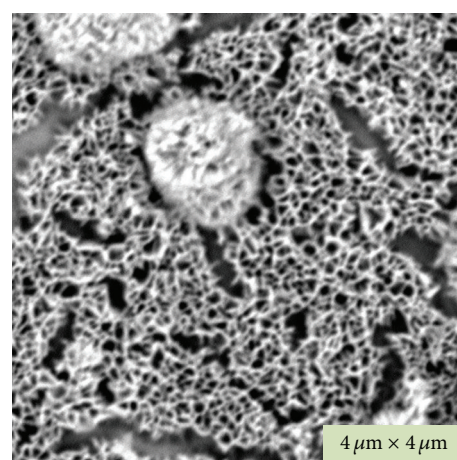
## 2. Experimental

All chemicals were of analytical reagent grade and used without further purification. Deionized water was used in each synthesis and in washing steps of both NiO and CuO layers' deposition. Nickel oxide (NiO) layers were deposited using chemical bath deposition (CBD) technique on precleaned indium tin oxide (ITO) coated glass plates. The precursor solution for NiO was obtained by dissolving 28.08 g (0.1 mol) of nickel sulfate hexahydrate ( $\text{NiSO}_4 \cdot 6\text{H}_2\text{O}$ ) and 5.42 g (0.02 mol) of potassium persulfate ( $\text{K}_2\text{S}_2\text{O}_8$ ) in 180 mL of deionized water. Clean ITO/glass substrates were immersed vertically in the solution, further of it; 30 mL of 30% ammonia solution was added. The mixture was maintained at 300 rpm stirring for approximately 30 minutes. Colour changes were observed in the solution upon addition of ammonia demonstrating the precipitation of nickel hydroxides particles [17, 18]. The obtained thickness of film varies in  $150 \pm 50$  nm range. After deposition, the substrate colour varied from grey to black depending on the thickness of the film. The samples were annealed in a furnace at 400°C for 1 hour to produce the desired NiO film and finally washed by sonication in ethanol for 2 minutes.

The synthesis of nanostructured rectangular horizontal pillars CuO layer on top of NiO porous layer was performed by applying the widely known hydrothermal method. For the growth process of CuO nanostructures, the freshly prepared NiO/ITO/glass substrate was submerged having face up in a 100 mL of 5 mM aqueous solution of copper nitrate trihydrate [ $\text{Cu}(\text{NO}_3)_2 \cdot 3\text{H}_2\text{O}$ ] and 1 mM of hexamethylenetetramine (HMT,  $\text{C}_6\text{H}_{12}\text{N}_4$ ) under constant stirring. A bluish solution was formed due the presence of copper ions. The solution



(a)



(b)

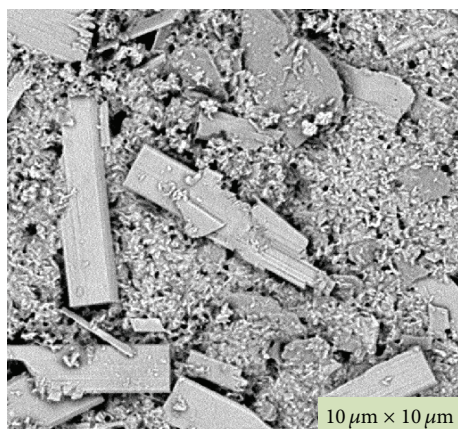
FIGURE 2: SEM images of NiO porous nanostructure deposited using chemical bath deposition on top of ITO coated glass plate.

was further heated using heating plate at 60°C for 4 hours. After the growth, the vessel was cooled down and a resulting black product of CuO nanopillars (Figure 3) was collected and washed several times with deionized water.

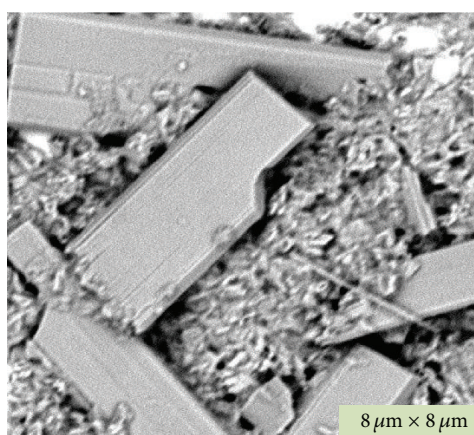
Microstructures of the nickel oxides and copper oxides were investigated by state-of-the-art techniques like X-ray diffractometer (XRD, Bruker D<sub>2</sub> Phaser system) with Cu K $\alpha$  radiation operating at 30 kV and 10 mA having wavelength ( $\lambda$ ) of 1.54 nm. For the morphological analysis, scanning electron microscopy (SEM, Phenom Desktop SEM, Phenom World, Netherland; 5 kV acceleration voltage) was carried out for nanostructure analysis of such inorganic layers. The optical transmission spectra of the samples were obtained in the ultraviolet (UV)/visible/near infrared (nir) region up to 1100 nm using Shimadzu UV-VIS spectrophotometer (Model: UV-3600).

## 3. Results and Discussion

Figure 2 shows the SEM micrographs of NiO thin film deposited at RT on ITO coated glass plate. AFM measurement (not



(a)



(b)

FIGURE 3: SEM images of CuO nanopillars/nanowalls-like structure deposited using hydrothermal method on top of NiO/ITO coated glass.

shown here) indicates that the thicknesses of such layers are in  $150 \pm 50$  nm range. It is observed that the film surface looks highly porous with some overgrown clusters and is composed of nanosized Ni crystallites. This overgrowth could be explained on the basis of nucleation and coalescence process. Similar porous structures growths of NiO have been reported also in literatures [19–22]. The porous NiO structure on ITO surface is uniformly distributed and grown along the entire ITO substrate as clearly shown in Figure 2(a).

Similarly, Figure 3 shows the top view of SEM micrographs of CuO nanostructured layer on NiO/ITO substrate. Different SEM images had been taken at various magnifications. From both pictures (Figure 3) one can clearly see the presence of nanowalls or thick nanopillars of rectangular shape structure, mostly lying horizontally and having average dimensions  $(5 \pm 1.0) \mu\text{m} \times (2.0 \pm 0.3) \mu\text{m}$ . At the same time one can clearly notice that the porous structures of NiO beneath CuO layer have been filled after depositing CuO layer on top of it. All the nanopillars are randomly oriented and distributed along the whole NiO film and they even

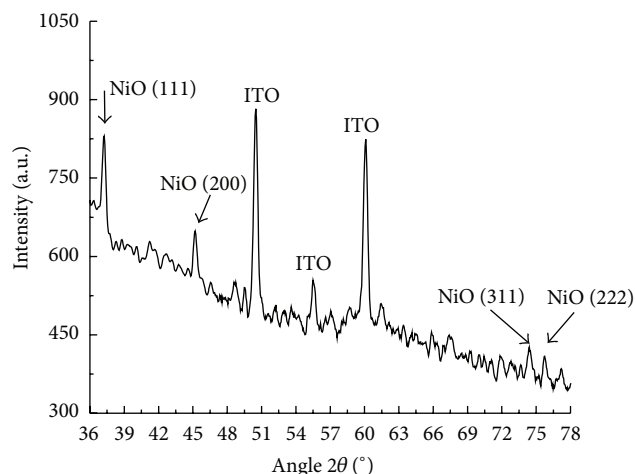


FIGURE 4: XRD scan of NiO film deposited using chemical bath deposition method on ITO glass, ITO peaks also noticed.

penetrated into the NiO surface. Similar morphologies have been reported, such as nanosheets, nanobelts, and wires [23–26].

Next, X-ray diffraction studies of NiO thin film on top of ITO layer had performed, particularly,  $\theta$ - $2\theta$  scan has taken in to account for all measurements, due to this buried substrate peaks are also visible in the scans. Figure 4 indicates the presence of NiO (111), NiO (200), NiO (311), and NiO (222) peaks, where NiO (111) and NiO (200) are the pronounced peaks. After exploiting Debye-Scherrer formula (size of crystallites =  $0.9\lambda/B^* \cos \theta$ , where  $B$  is peak width in radian) as well as interplanar distance ( $D$  spacing =  $\lambda/2 \sin \theta$ ), it has been observed that both peaks show similar size of crystallites along the surface normal direction. Relatively NiO (111) peak area is doubled to NiO (200); this indicates that NiO (111) orientation is dominating in the NiO film (Table 1). At the same time numbers of NiO (111) crystallites are doubled compared to NiO (222) crystallites along the whole depth of the film.

Figure 5 shows the XRD curve of CuO film deposited on NiO/ITO substrate using hydrothermal method. One can observe multiple peaks which correspond to random orientation of CuO crystallites, of which (002) phase has the highest intensity indicating the maximum number of such crystallites present in CuO thin films along the surface normal direction, whereas CuO (200)/(111) is the second highest in intensity.

All the peak values calculated from Debye-Scherrer formula and interplanar distances have been summarized in Table 2; one can see that due to the least full width half maximum of CuO (–110) peak ( $0.281^\circ$ ), the biggest size of crystallites observed is of CuO (–110) of 29 nm. At the same time CuO (002) has the size of crystallites along surface normal direction which is 16 nm. CuO (002), CuO (200), and CuO (–202) have almost the same full width at half maximum and size of the crystallites.

TABLE 1: Different calculated values corresponding to Ni (111) and Ni (220) pronounced peaks observed in XRD scan of NiO/ITO sample.

Peaks	FWHM (degree)	Position (degree)	Area (Arb.)	D spacing (nm)	Size of crystallites (nm)
Ni (111)	0.369	37.23	67	0.241	26
Ni (220)	0.331	45.20	30	0.205	29

TABLE 2: Calculated values corresponding to some of the CuO pronounced peaks observed in XRD scan of CuO/NiO/ITO sample.

Peaks	FWHM (degree)	Position (degree)	Area (Arb.)	D spacing (nm)	Size of crystallites (nm)
CuO (-110)	0.281	30.18	483	0.30	29
CuO (002)	0.516	35.23	2330	0.26	16
CuO (111)/CuO (200)	0.449	38.56	1630	0.23	19
CuO (-202)	0.531	48.55	315	0.19	16

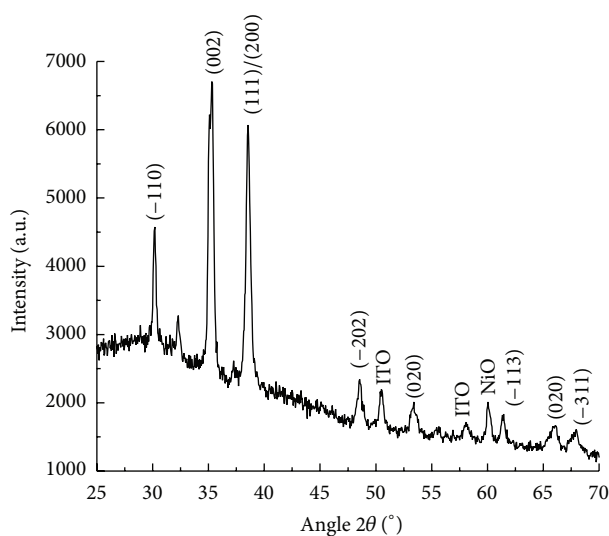


FIGURE 5: XRD scan of CuO thin film on top of NiO/ITO substrate deposited using hydrothermal method on ITO glass; some of ITO and NiO peaks are also noticed.

For the optical properties, UV spectroscopy has been utilized to study the different layers (CuO/NiO). Figure 6 shows the transmittance spectra of nanostructured NiO thin film on ITO substrate. One can see that the transmittance is increasing with the wavelength, no additional peak has been observed in between the whole range, and a continuous increasing spectrum has been observed. It indicates that under UV region the sample has the absorption peak at 280 nm and absorbs the UV light, whereas under the visible region (400–750 nm) the sample becomes more transparent towards higher wavelengths.

The CuO layer UV curve is shown in Figure 7. From Figure 7 it is clearly visible that except for low wavelengths (200–350 nm) the absorption is increasing toward higher wavelengths, which is opposite to NiO layer property.

In the visible range (400–750 nm), the maximum absorption is obtained around 700 nm. This shows that the film is highly active towards the higher wavelengths. The energy band gap ( $E_g$ ) was estimated by assuming a direct transition between valence and conduction bands from the expression  $\alpha h\nu = k(h\nu - E_g)^{1/2}$ , where  $k$  is constant and  $E_g$  is determined by extrapolating the straight line portion of the spectrum to  $\alpha h\nu = 0$ . Using this, the NiO and CuO band gaps have estimated 2.78 eV and 1.80 eV, respectively.

#### 4. Conclusions

We have explored chemical bath deposition (CBD) as well as the hydrothermal deposition techniques for growing the nanostructures of NiO and CuO inorganic materials. These nanostructures of copper oxide (CuO) and nickel oxide (NiO) have great potential for applications in the fields of optoelectronics and sensor devices. Surface morphology of both films (NiO, CuO) has been studied by state-of-the-art techniques like SEM, XRD, and UV. NiO thin film reveals the porous structure, whereas CuO layer has shown nanopillars/nanowalls-like structure. By judiciously manipulating the deposition conditions, the mean ledge thickness of the NiO and CuO nanopillars can be controlled. The crystalline properties and growth direction of as-synthesized NiO and CuO nanostructures were studied by XRD and SEM techniques; it confirms the polycrystalline phase and surface normal direction of their most preferred direction of growth for CuO nanopillars.

The present work primarily covers NiO and CuO nanostructures thin films formation, study of their low temperature growth. The layer combination ITO/NiO/CuO is completely open to put any n-type layer for application as a pn-junction like photovoltaics, sensors, and so forth. These big nanopillars of CuO films can make a difference in terms of device performance (charge transport), if used properly with suitable n-type materials. Further work of these structures towards solar cells and humidity sensors is in progress.

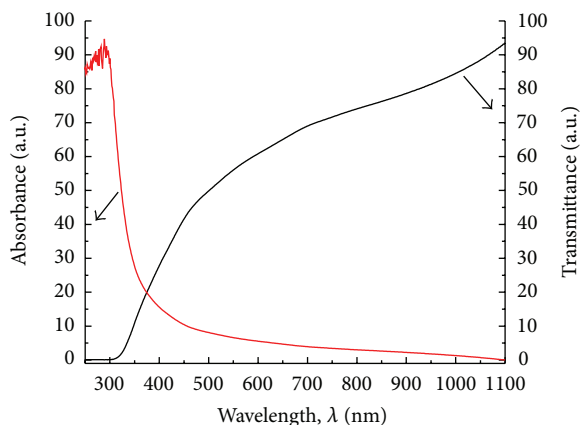


FIGURE 6: UV transmission and absorbance curve of NiO film deposited on ITO substrate using chemical bath deposition process.

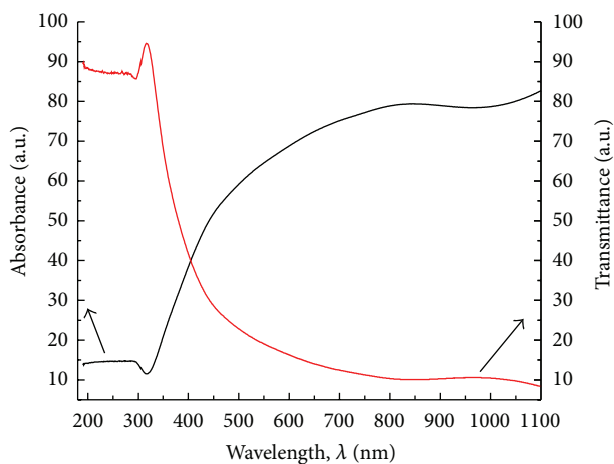


FIGURE 7: UV transmission and absorbance curve of CuO film deposited on NiO/ITO substrate using hydrothermal method.

## Conflict of Interests

The authors declare that there is no conflict of interests regarding the publication of this paper.

## Acknowledgments

This work was supported by the Department of Science and Technology (DST) under Nano Mission programme; the authors greatly appreciate the financial support from DST, India.

## References

- [1] A. I. Hochbaum and P. Yang, "Semiconductor nanowires for energy conversion," *Chemical Reviews*, vol. 110, no. 1, pp. 527–546, 2010.
- [2] M. Law, J. Goldberger, and P. Yang, "Semiconductor nanowires and nanotubes," *Annual Review of Materials Research*, vol. 34, no. 1, pp. 83–122, 2004.
- [3] Z. Fan, D. J. Ruebusch, A. A. Rathore et al., "Challenges and prospects of nanopillar-based solar cells," *Nano Research*, vol. 2, no. 11, pp. 829–843, 2009.
- [4] L. Cao, J. Park, P. Fan, B. Clemens, and M. L. Brongersma, "Resonant germanium nanoantenna photodetectors," *Nano Letters*, vol. 10, no. 4, pp. 1229–1233, 2010.
- [5] J. Xiang, W. Lu, Y. Hu, Y. Wu, H. Yan, and C. M. Lieber, "Ge/Si nanowire heterostructures as high-performance field-effect transistors," *Nature*, vol. 441, no. 7092, pp. 489–493, 2006.
- [6] W. Shi, S. Song, and H. Zhang, "Hydrothermal synthetic strategies of inorganic semiconducting nanostructures," *Chemical Society Reviews*, vol. 42, no. 13, pp. 5714–5743, 2013.
- [7] C. N. R. Rao and A. Govindaraj, "Synthesis of inorganic nanotubes," *Advanced Materials*, vol. 21, no. 42, pp. 4208–4233, 2009.
- [8] J. Yu, F. Wang, Y. Wang, H. Gao, J. Li, and K. Wu, "Interfacial reaction growth approach to preparing patterned nanomaterials and beyond," *Chemical Society Reviews*, vol. 39, no. 5, pp. 1513–1525, 2010.
- [9] P. Yang, R. Yan, and M. Fardy, "Semiconductor nanowire: whats next?" *Nano Letters*, vol. 10, no. 5, pp. 1529–1536, 2010.
- [10] J. Jie, W. Zhang, I. Bello, C. Lee, and S. Lee, "One-dimensional II-VI nanostructures: synthesis, properties and optoelectronic applications," *Nano Today*, vol. 5, no. 4, pp. 313–336, 2010.
- [11] M. Faisal, S. B. Khan, M. M. Rahman, A. Jamal, and A. Umar, "Ethanol chemi-sensor: Evaluation of structural, optical and sensing properties of CuO nanosheets," *Materials Letters*, vol. 65, no. 9, pp. 1400–1403, 2011.
- [12] X. Jiang, W. Huang, H. Li, and X. Zheng, "Catalytic properties of CuO/Ce<sub>0.2</sub>Ti<sub>0.8</sub>O<sub>2</sub> and CuO/Ce<sub>0.5</sub>Ti<sub>0.5</sub>O<sub>2</sub> in the NO + CO reaction," *Energy Fuels*, vol. 24, pp. 261–266, 2009.
- [13] D. Li, Y. H. Leung, A. B. Djurišić et al., "CuO nanostructures prepared by a chemical method," *Journal of Crystal Growth*, vol. 282, no. 1-2, pp. 105–111, 2005.
- [14] G. Gao, H. Wu, M. Chen, L. Zhang, B. Yu, and L. Xiang, "Synthesis of size- and shape-controlled CuO assemblies," *Journal of the Electrochemical Society*, vol. 158, no. 3, pp. K69–K73, 2011.
- [15] L. C. Olsen, R. C. Bohara, and M. W. Urie, "Explanation for low-efficiency Cu<sub>2</sub>O Schottky-barrier solar cells," *Applied Physics Letters*, vol. 34, no. 1, pp. 47–50, 1979.
- [16] J. Herion, E. A. Niekisch, and G. Scharl, "Investigation of metal oxide/cuprous oxide heterojunction solar cells," *Solar Energy Materials*, vol. 4, no. 1, pp. 101–112, 1980.
- [17] M. Izaki, K. Mizuno, T. Shinagawa, M. Inaba, and A. Tasaka, "Photochemical construction of photovoltaic device composed of p-copper(I) oxide and n-zinc oxide," *Journal of the Electrochemical Society*, vol. 153, no. 9, pp. C668–C672, 2006.
- [18] M. Izaki, T. Shinagawa, K. Mizuno, Y. Ida, M. Inaba, and A. Tasaka, "Electrochemically constructed p-Cu<sub>2</sub>O/n-ZnO heterojunction diode for photovoltaic device," *Journal of Physics D: Applied Physics*, vol. 40, no. 11, article 010, pp. 3326–3329, 2007.
- [19] H. Huang, J. Tian, W. K. Zhang et al., "Electrochromic properties of porous NiO thin film as a counter electrode for NiO/WO<sub>3</sub> complementary electrochromic window," *Electrochimica Acta*, vol. 56, no. 11, pp. 4281–4286, 2011.
- [20] U. M. Patil, R. R. Salunkhe, K. V. Gurav, and C. D. Lokhande, "Chemically deposited nanocrystalline NiO thin films for supercapacitor application," *Applied Surface Science*, vol. 255, no. 5, pp. 2603–2607, 2008.

- [21] G. Cai, J. Tu, J. Zhang et al., "An efficient route to a porous NiO/reduced graphene oxide hybrid film with highly improved electrochromic properties," *Nanoscale*, vol. 4, no. 18, pp. 5724–5730, 2012.
- [22] X. H. Xia, J. P. Tu, J. Zhang, X. L. Wang, W. K. Zhang, and H. Huang, "Morphology effect on the electrochromic and electrochemical performances of NiO thin films," *Electrochimica Acta*, vol. 53, no. 18, pp. 5721–5724, 2008.
- [23] M. A. Dar, Q. Ahsanulhaq, Y. S. Kim, J. M. Sohn, W. B. Kim, and H. S. Shin, "Versatile synthesis of rectangular shaped nanobattle-like CuO nanostructures by hydrothermal method; structural properties and growth mechanism," *Applied Surface Science*, vol. 255, no. 12, pp. 6279–6284, 2009.
- [24] Y. Xu, D. Chen, and X. Jiao, "Fabrication of CuO prickly microspheres with tunable size by a simple solution route," *Journal of Physical Chemistry B*, vol. 109, no. 28, pp. 13561–13566, 2005.
- [25] H. Xu, W. Wang, W. Zhu, L. Zhou, and M. Ruan, "Hierarchical-oriented attachment: from one-dimensional Cu(OH)<sub>2</sub> nanowires to two-dimensional CuO nanoleaves," *Crystal Growth and Design*, vol. 7, no. 12, pp. 2720–2724, 2007.
- [26] H. Yu, J. Yu, S. Liu, and S. Mann, "Template-free hydrothermal synthesis of CuO/Cu<sub>2</sub>O composite hollow microspheres," *Chemistry of Materials*, vol. 19, no. 17, pp. 4327–4334, 2007.



**Hindawi**

Submit your manuscripts at  
<http://www.hindawi.com>

